https://doi.org/10.2352/ISSN.2470-1173.2020.15.COLOR-351

Developing an inkjet printer II : CMY ink amounts to multibit CMY halftones*

***Baekdu Choi*[1]*, Daulet Kenzhebalin*[1]*, Sige Hu*[1]*, George Chiu*[1]*, Davi He*[2]*, Zillion Lin*[2] *and Jan P. Allebach*[1]**
[1] ***Electronic Imaging Systems Laboratory, School of Electronic and Computer Engineering, Purdue University, West Lafayette, IN 47907, US; choi504, dkenzheb, hu539, gchiu, allebach@purdue.edu***
[2] ***Sunvalleytek International Inc., Shenzhen, CHINA***

Abstract

In this paper, we propose a novel error diffusion halftoning algorithm for the conversion of cyan, magenta and yellow (CMY) ink amounts to a multi-bit halftone image. We adopt the idea of allowing multiple drops of colorants in order to achieve print results with better saturation, which is implemented by modifying the classic Floyd-Steinberg error diffusion algorithm. For better halftone texture and more efficient use of colorants, we add a dot-off-dot feature to the classic Floyd-Steinberg error diffusion. Blending-in the original input image with its DBS screened multi-level halftone image as a preprocessing step to dot-off-dot error diffusion is proposed as a measure to reduce halftone artifacts. Digitally simulated halftone images will be presented to illustrate the better halftone texture that can be achieved by applying the proposed algorithm.

Introduction

Digital color halftoning processes a given continuous-tone input image into an image with a limited number of colors [1]. Halftoning algorithms can be classified based on two criteria, whether the dot placement is periodic or aperiodic, and whether they are clustered-dot or dispersed-dot halftoning algorithms. All four possible combinations are known to be employed in practice [2]. The algorithm we propose in this paper can be classified as an aperiodic dispersed-dot halftoning algorithm.

Halftoning algorithms can also be classified based on their computational complexity. The least computationally expensive type is screening, where each pixel of the input image is compared to the corresponding index of a halftone screen to determine the value of the pixel in the halftone image. Well-known algorithms to generate the screen include the void and cluster algorithm in [3] and the direct binary search (DBS) based screen generating algorithm in [4], the latter of which we will be using for our algorithm.

Another type of halftoning algorithm which tends to be slightly more complicated is error diffusion. Here, an image is quantized first, and the error between the pixel value of the input image and that of the halftone image is diffused to nearby pixels. Error diffusion was first introduced by Floyd and Steinberg in [5]. Our proposed algorithm will fall into the category of error diffusion algorithms.

The most complex type of the halftoning algorithm involves searching through the image to optimize a cost function, such as direct binary search (DBS) algorithm in [6]. While this type of algorithm tends to generate the best quality halftone images, using DBS to generate a halftone image could take a significant amount of time, for instance as shown by Liao in [7]. Li and Allebach proposed tone-dependent error diffusion [8] which provides a method to generate halftone images with quality comparable to those generated with DBS but with the complexity of error diffusion algorithms, by varying the filter weights and thresholds of the error diffusion algorithm, based on the input pixel value.

Color image halftoning has also been a topic of interest in multiple studies. For instance, Monga et al. [9] proposed an extension to [8] for color images. Color printing presents challenges such as visibility of overlapping colorant drops, which results in deteriorated texture of the halftone print. Therefore DBS-based color halftoning with the goal to minimize the overlap between colorants were proposed in papers such as Lee and Allebach [10], Agar and Allebach [11], and He [12]. Schramm and Gondek proposed tone-dependent, plane-dependent error diffusion [13] where the combined tone of the color planes is used to determine the threshold levels and error weights used for each color plane when performing color error diffusion. A recent work with color image halftoning that could be of interest is the work of Jiang et al. [14], where the color image is converted into what is known as a Neugebauer Primary Area Coverage (NPAC) image, and then swap-only DBS is performed.

While a majority of the work about halftoning is on bi-level halftoning, there has been work on multi-level halftoning as well. Elias et al. [15] introduced a multi-level printing process by adding four more channels (light cyan, light magenta, gray, photo gray, and gray) to the conventional *CMYK* (cyan, magenta, yellow and black) printing to result in eight-channel printing. Lin and Allebach [16] discussed the use of a DBS screen with the goal of reducing contours that occur when multilevel screening is naively implemented. Chandu et al. [17] proposed an extension to DBS that they refer to as direct multi-bit search (DMS) to generate a multi-level screen. Multi-level halftoning enables us to perform multi-drop printing, which in an inkjet printer is implemented by simply locating multiple drops at a single printer-addressable pixel [18]. This will give us a wider printer gamut, including more saturated colors that can be printed, which is desirable for our application.

In this paper, we propose a novel error diffusion algorithm for multi-level color halftoning. The paper is organized as follows. First, we discuss how the bi-level error diffusion algorithm in [5] can be extended to multi-level halftoning. The simple extension independently processes each color plane of the input image. But this does not give us a method to control the amount of

* Research supported by Sunvalleytek Internation Inc., Shenzhen, CHINA

overlap of colorant drops, which tend to be highly visible, thus degrading the texture of the halftone image. To address this issue, we propose a dot-off-dot halftoning method, which will result in reduced overlap of the colorant drops. Finally, a preprocessing step for the error diffusion algorithm that gets rid of the artifacts in the halftone image commonly associated with error diffusion is proposed. For each section in the paper, halftone images will be compared in order to illustrate the effects of the proposed algorithm.

2-drop error diffusion

We start with a simple extension of the Floyd-Steinberg error diffusion algorithm in [5], which is a one-drop halftoning algorithm. We will first describe it for a single-channel monochrome image, and later discuss the extension to color. Analogous to the Floyd-Steinberg error diffusion algorithm, we keep track of the *error diffused image*, which is initialized as a copy of the original input image $f[m,n]$. Here, we assume that $0 \leq f[m,n] \leq 1$, where 0 denotes white and 1 denotes black. Let us denote the error diffused image as $\tilde{f}[m,n]$ where the brackets $[\cdot]$ indicate that the pixel locations are discretized. For each pixel in one color plane of the error diffused image, we quantize the pixel value of $\tilde{f}[m,n]$ and assign corresponding values to the tri-level halftone image $g[m,n]$ by :

$$g[m,n] = \begin{cases} 0, & \text{if } \tilde{f}[m,n] < \frac{1}{3} \\ \frac{1}{2}, & \text{if } \frac{1}{3} \leq \tilde{f}[m,n] < \frac{2}{3} \\ 1, & \text{if } \tilde{f}[m,n] \geq \frac{2}{3} \end{cases} \tag{1}$$

Note that the pixel values for $g[m,n]$, 0, $\frac{1}{2}$ and 1, represents 0, 1 and 2 drops of colorant, respectively. After the quantization step, the error between the error diffused image and the halftone image is computed and diffused to nearby pixels in the error diffused image as

$$e[m,n] = \tilde{f}[m,n] - g[m,n] \tag{2}$$

$$\tilde{f}[m+k,n+l] \leftarrow \tilde{f}[m+k,n+l] + e[m,n]h[k,l] \tag{3}$$

where

$$h[k,l] = \frac{7}{16}\delta[k,l-1] + \frac{3}{16}\delta[k-1,l+1] + \frac{5}{16}\delta[k-1,l] + \frac{1}{16}\delta[k-1,l-1] \tag{4}$$

is same as the error diffusion filter for [5].

For our work, the serpentine raster has been chosen as the direction in which the scan is performed for the image. When performing a serpentine raster scan, the image is first scanned in the first row from the left to the right. As we proceed to the next row, instead of starting from the first column again, we alternate the scan direction; e.g., for the second row, we scan from the rightmost column and proceed to the left. Serpentine raster scan is known to reduce halftone artifacts associated with error diffusion ([19], pg. 266). But at the same time, its effect tends to be rather limited, especially with vertical artifacts ([20], pg. 374). As an illustration, consider Figures 2, 3, 5 and 6; it is easily noticed that the halftone images contain unwanted vertical artifacts and thus are not suitable reproductions of the original images.

Dot-off-dot 2-drop error diffusion

The previously implemented 2-drop error diffusion processes each color plane in cyan, magenta and yellow (CMY) independently. However, it is more desirable to locate the colorant drops on different pixel locations than to locate them on top of each other, which is commonly known as *dot-off-dot* halftoning. Dot-off-dot halftoning has the following potential benefits: First, it could result in using less ink compared to overlapping the colorant drops, since it reduces interaction between the colorant drops. A discussion of similar effects can be found in [18].

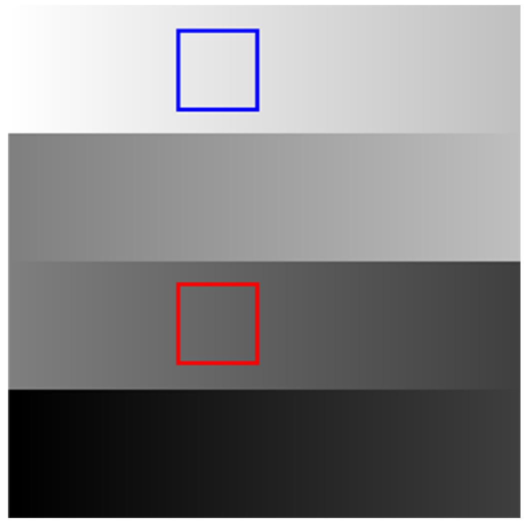

Figure 1. *Original input image 1 to be halftoned. While this image is in the sRGB color space, $R = G = B$ for all the pixels; so the image looks monochrome. The blue and red box are not parts of the original image; they are used to illustrate which part of the image will be magnified for Figures 2 and 9.*

Figure 2. *Magnified view of the red box area of Figure 1. In CMY color space, the absorptance values slowly increase from $C = M = Y = 0.616$ to $C = M = Y = 0.655$ from left to right. Conversion from sRGB color space to CMY color space was performed with the simple conversion formula $C = 1-R, M = 1-G, Y = 1-B$.*

Second, it could result in halftone images with smoother texture, since we reduce the number of overlapping drops which tend to be more visible compared to single drops of colorants.

We propose a way to perform dot-off-dot 2-drop halftoning by limiting the number of all colorant drops possible for each pixel. Our proposed algorithm first looks at the sum of the color planes at the current pixel. Based on the sum, it de-

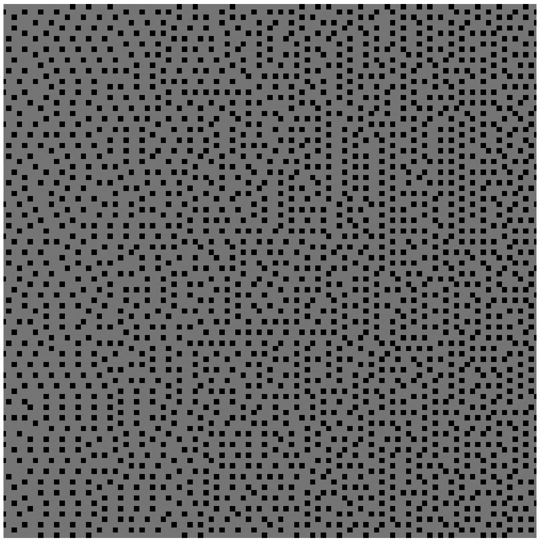

Figure 3. *Halftoned image of Figure 2 using the 2-drop error diffusion algorithm. Note that the image contains only gray and black pixels even though the halftoning algorithm uses three colorants C,M,Y and not K. This is because all the pixels in Figure 2 have the same absorptance values in CMY color space, and since the simple 2-drop error diffusion algorithm halftones each color plane independently, the halftones for each color plane are identical to each other. Therefore, when they are combined together, the colorants all overlap and end up as pixels with monochromatic colors. The gray pixels are the overlap of one drop of all the colorants; and the black pixels are the overlap of two drops of all the colorants.*

Figure 4. *Original input image 2 to be halftoned. The red box is not a part of the original image. It is used to illustrate which part of the image will be magnified for Figure 5.*

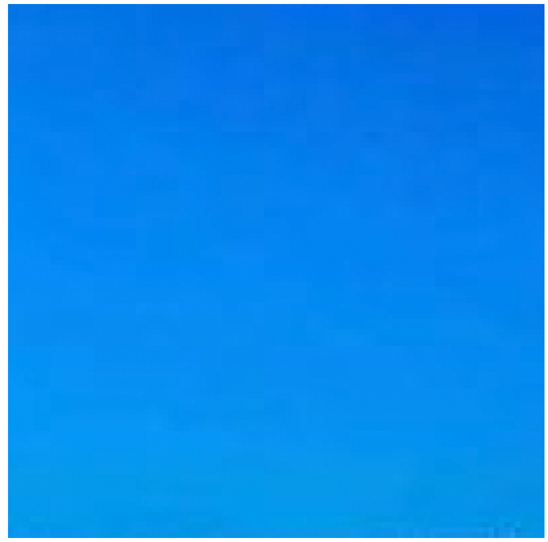

Figure 5. *Magnified view of the red box area of Figure 4. In CMY color space, the image consists of cyan pixels with absorptance values of almost 1, and magenta pixels with absorptance values around 0.5. The yellow pixels have absorptance values around 0.06. The magenta level decreases from around 0.569 to around 0.412 from top to bottom. Conversion from sRGB color space to CMY color space was performed with the simple conversion formula $C = 1-R, M = 1-G, Y = 1-B$.*

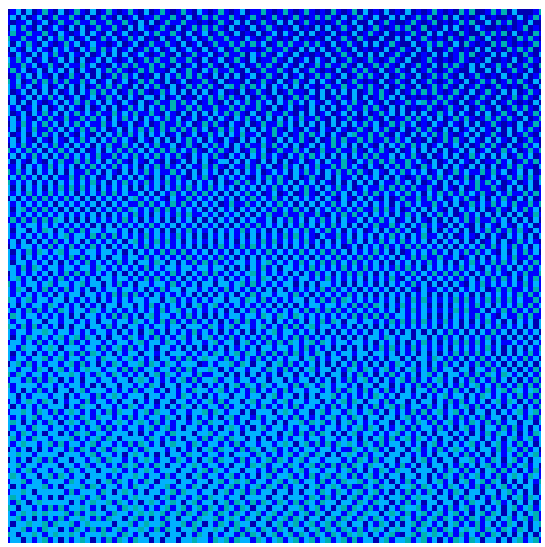

Figure 6. *Halftoned image of Figure 5 using the 2-drop error diffusion algorithm. The halftone image mostly consist of four different pixels - light green, light blue, medium blue, and dark blue. Light green pixels are the overlap of two drops of cyan, one drop of magenta, and one drop of yellow. While the combination of drops of colorants for the light green pixel should appear as desaturated cyan, it appears light green in this image since it is surrounded by more saturated blueish colored pixels. When the color is isolated it appears to be desaturated cyan as expected. Light blue pixels are the overlap of two drops of cyan and one drop of magenta. Medium blue pixels are the overlap of two drops of cyan and magenta. Dark blue pixels are the overlap of two drops of cyan, two drops of magenta, and one drop of yellow.*

termines the maximum number of all colorant drops to locate at the pixel. The maximum number of colorant drops with respect to the sum of color planes is defined in Eq. (5). We denote $\tilde{f}[m,n] = \tilde{f}_C[m,n] + \tilde{f}_M[m,n] + \tilde{f}_Y[m,n]$ as the sum of the color planes.

$$N_{drops} = \begin{cases} 1, & \text{if } \tilde{f}[m,n] < \frac{2}{3} \\ 2, & \text{if } \frac{2}{3} \leq \tilde{f}[m,n] < \frac{4}{3} \\ 3, & \text{if } \frac{4}{3} \leq \tilde{f}[m,n] < 2 \\ 4, & \text{if } 2 \leq \tilde{f}[m,n] < \frac{8}{3} \\ 5, & \text{if } \frac{8}{3} \leq \tilde{f}[m,n] < 3 \\ 6, & \text{if } \tilde{f}[m,n] \geq 3 \end{cases} \tag{5}$$

After determining the maximum possible number of drops for the pixel, the pixel is quantized in the same way as shown in Eq. (1). However, since we have put a limit on the maximum number of all colorant drops, the order of the quantization matters, and the color plane with the largest absorptance should be quantized first. For this, at each pixel, the color planes are ranked from the highest absorptance level to lowest absorptance level. Then, we quantize the color planes in the order of decreasing rank using Eq. (1). But the allocation of the colorant drops is limited by the leftover number of drops, which is the difference between the maximum number of drops and the number of drops already allocated from processing the color planes with higher rank at the current pixel. After allocating the colorant drops, the diffusion of the error is performed in the same way as with the previously discussed algorithm, mainly according to Eq. (2) and Eq. (3) using the filter described in Eq. (4). Limiting the number of drops for each pixel is the main factor that results in dot-off-dot halftoning.

For the sake of naming, we will refer to the 2-drop halftoning algorithm without the dot-off-dot property as the *simple* 2-drop error diffusion algorithm from now on. Comparing Figures 2 and 3 with Figure 7, we can see that dot-off-dot halftoning indeed produces smoother halftone texture and less visible artifacts compared to the simple 2-drop halftoning algorithm. Comparing Figures 5 and 6 with Figure 8 leads to a similar conclusion.

However, dot-off-dot halftoning has a limitation that not all the artifacts are removed. To illustrate, consider Figures 9, 10 and 11. Comparing the halftone images, we can easily see that the halftone image generated by the dot-off-dot error diffusion has vertical structured artifacts in the left of center region of the image, which are similar to those that appear in the halftone image generated with the simple 2-drop error diffusion algorithm. Furthermore, dot-off-dot 2-drop error diffusion has a fundamental limit that if one color plane component in the image is predominant and has much larger absorptance values compared to the other two color plane components, the dot-off-dot strategy will not have much effect on the quality of the resulting halftone image. If we consider an extreme case where only one color plane component has nonzero absorptance values, dot-off-dot 2-drop error diffusion will become simple 2-drop error diffusion, and thus all the artifacts will still remain in the resulting halftone image.

DBS screen blending-in

The direct binary search (DBS) algorithm introduced in [6] is known to generate high-quality halftone images. Since the DBS algorithm is computationally expensive, it cannot be used for the printer we are developing. One way to take advantage of the DBS algorithm is to use a DBS-generated screen. The method for generating a DBS screen can be found in [4]. Using a DBS-generated screen to halftone a continuous-tone image will eliminate the artifacts commonly associated with error diffusion, but the resulting halftone images tend to be considerably noisier than those result-

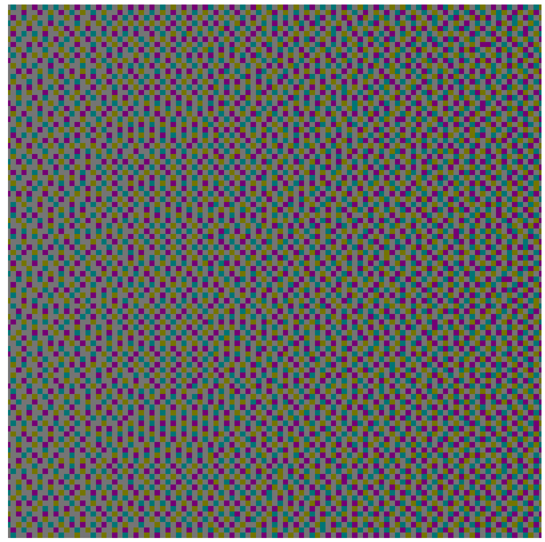

Figure 7. *Halftoned image of Figure 2 using the dot-off-dot 2-drop error diffusion algorithm. Note that compared to Figure 3, this halftone image contains pixels with colors such as dark cyan, dark magenta and dark yellow along with gray pixels. This is because dot-off-dot error diffusion tries to discourage colorants from overlapping with each other. The dark cyan pixel is the overlap of two cyan drops, one magenta drop and one yellow drop. The dark magenta pixel is the overlap of one cyan drop, two magenta drops and one yellow drop. The dark yellow pixel is the overlap of one cyan drop, one magenta drop and two yellow drops. As in Figure 3, the gray pixels are the overlap of one drop of each colorant.*

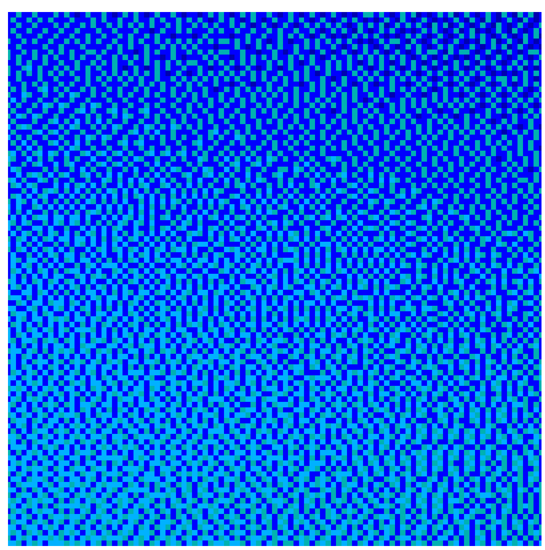

Figure 8. *Halftoned image of Figure 5 using the dot-off-dot 2-drop error diffusion algorithm. Compared to Figure 6, the vertical line artifacts that span the image horizontally in the middle region of Figure 6 do not appear in this figure.*

ing from error diffusion.

Here, we propose DBS screen blending-in as a preprocessing step prior to dot-off-dot error diffusion to find a compromise between the noisiness of the screened halftone images and the artifacts associated with error diffused halftone images. The procedure for applying DBS screen blending-in to generate halftone images is as follows: First, for each color plane CMY of the original continuous-tone image f_c, f_m and f_y, we apply a tri-level DBS screen to obtain tri-level halftone images $\tilde{g}_c$, $\tilde{g}_m$ and $\tilde{g}_y$. For the three color planes CMY, we obtain mixtures $\tilde{f}_c$, $\tilde{f}_m$ and $\tilde{f}_y$ of the tri-level screened image and the original continuous-tone image following Eq. (6). After that, we perform dot-off-dot 2-drop halftoning on $\tilde{f}$.

Figure 9. Magnified view of the blue box area of Figure 1. In CMY color space, the absorptance values slowly increase from $C = M = Y = 0.106$ to $C = M = Y = 0.153$ from left to right. Conversion from sRGB color space to CMY color space was performed with the simple conversion formula $C = 1-R, M = 1-G, Y = 1-B$.

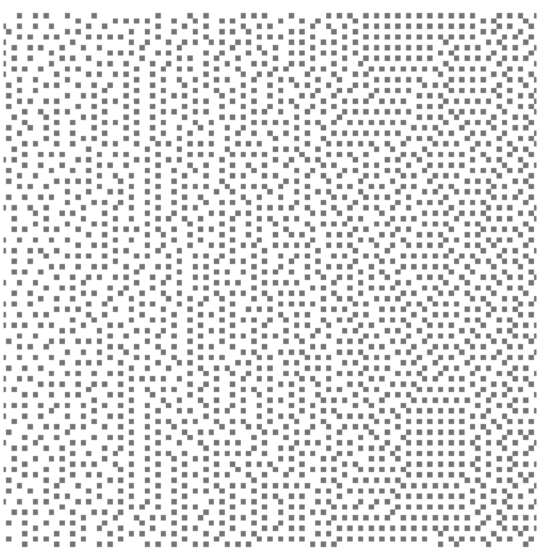

Figure 10. Halftoned image of Figure 9 using the simple 2-drop error diffusion algorithm. Similar to Figure 3, the colorants overlap for all gray pixels and end up looking monochromatic.

$$\tilde{f}_k[m,n] = 0.8 \cdot f_k[m,n] + 0.2 \cdot \tilde{g}_k[m,n],\ k \in \{C,M,Y\} \tag{6}$$

To use the DBS screen for tri-level screening, we first start with a set of three different bilevel DBS screens, one for each colorant C, M, and Y, generated following the method explained in [4]. Let us denote one color plane among CMY of the original continuous-tone input image as $f[m,n]$, the bi-level DBS screen of size $N_s \times N_s$ as $s[m,n]$, and the resulting tri-level halftone image as $\tilde{g}[m,n]$. As before, we assume that the continuous-tone input image and the screen are normalized so that all the elements are in the range $[0,1]$. First, we divide the screen $s[m,n]$ by 2 and use the resulting scaled screen to halftone the image to generate a bilevel halftone image $\tilde{g}_1[m,n]$ as in Eq. (7) :

$$\tilde{g}_1[m,n] = \begin{cases} 1, & \text{if } f[m,n] \geq 0.5 \cdot s[m \bmod N_s, n \bmod N_s] \\ 0, & \text{otherwise} \end{cases} \tag{7}$$

The operator mod stands for the modulo operation. Then, we subtract 0.5 from each pixel of $f[m,n]$, and use the same scaled screen again to halftone the image to generate another bilevel halftone image $\tilde{g}_2[m,n]$ as in Eq. (8) :

$$\tilde{g}_2[m,n] = \begin{cases} 1, & \text{if } f[m,n] - 0.5 \geq 0.5 \cdot s[m \bmod N_s, n \bmod N_s] \\ 0, & \text{otherwise} \end{cases} \tag{8}$$

The last step for generating a tri-level screened image is to combine $\tilde{g}_1$ and $\tilde{g}_2$ to generate $\tilde{g}$ simply by letting $\tilde{g}[m,n] = 0.5 \cdot$

Figure 11. Halftoned image of Figure 9 using the dot-off-dot 2-drop error diffusion algorithm. Six different colors in addition to white are observed - light cyan, light magenta, light yellow, light red, light blue and light green. Light cyan, magenta and yellow are single drops of each colorant with no other colorants overlapping. Light red is the overlap of one drop of magenta and one drop of yellow. Light green is the overlap of one drop of cyan and one drop of yellow. Light blue is the overlap of one drop of cyan and one drop of magenta.

$\tilde{g}_1[m,n] + 0.5 \cdot \tilde{g}_2[m,n]$. As mentioned earlier, we use a different screen for each color plane of CMY, which will have an effect somewhat similar to that of dot-off-dot halftoning.

Combining the DBS screen blending-in with the dot-off-dot 2-drop error diffusion, the entire algorithm proposed in this paper can be summarized as in Algorithm 1. In the algorithm, f_C, f_M and f_Y refer to the continuous-tone color planes CMY of the original input image, and s_C, s_M and s_Y refer to the DBS screens to be used for screening each CMY color plane, respectively. The image size is denoted as $Ny \times N_x$, where N_y is the number of rows and N_x is the number of columns, and the screen size is $N_s \times N_s$.

To illustrate that the algorithm is working as intended, we now present the halftoned images. Figures 12, 13, and 14 are the halftone images of Figures 9, 2, and 5, respectively, resulting from DBS screen blending-in and dot-off-dot error diffusion. Comparing the halftone images to the other halftone images included in this paper, we can draw two conclusions: First, the halftone images produced with DBS screen blending-in and dot-off-dot error diffusion do not seem to contain most of the artifacts associated with error diffusion. And second, the halftone images produced with DBS screen blending-in and dot-off-dot error diffusion have smoothness comparable to halftone images generated with simple 2-drop error diffusion or dot-off-dot 2-drop error diffusion without DBS screen blending-in.

Figure 12. Halftoned image of Figure 9 using DBS screen blending-in and dot-off-dot 2-drop error diffusion algorithm.

Conclusions

In this paper, we proposed a new halftoning algorithm that generates good quality halftone images. We started with a 2-drop error diffusion algorithm, which is a simple extension of Floyd-Steinberg error diffusion. Halftone images generated with this simple 2-drop error diffusion algorithm tend to show artifacts typically associated with error diffusion. Then dot-off-dot 2-drop error diffusion halftoning was proposed with the goal of ink savings and smoother halftone textures. While dot-off-dot 2-drop error diffusion somewhat alleviates the artifacts seen with standard 1-drop Floyd-Steinberg error diffusion using a serpentine raster, the effect was found to be rather limited. To address this issue, DBS

Algorithm 1 The overall proposed halftoning algorithm including all the steps.

for $m = 0$ to $N_y - 1$ **do**
  for $n = 0$ to $N_x - 1$ **do**
    for $k \in \{C, M, Y\}$ **do**
      if $f_k[m,n] \geq 0.5 s_k[m \bmod N_s, n \bmod N_s]$ **then**
        $\tilde{g}_{k1}[m,n] = 1$
      else
        $\tilde{g}_{k1}[m,n] = 0$
      end if
      if $f_k[m,n] - 0.5 \geq 0.5 s_k[m \bmod N_s, n \bmod N_s]$ **then**
        $\tilde{g}_{k2}[m,n] = 1$
      else
        $\tilde{g}_{k2}[m,n] = 0$
      end if
      $g_k[m,n] = 0.5\tilde{g}_{k1}[m,n] + 0.5\tilde{g}_{k2}[m,n]$
      $\tilde{f}_k[m,n] = 0.8 f_k[m,n] + 0.2 g_k[m,n]$
    end for
  end for
end for
for $m = 0$ to $N_y - 1$ **do**
  if $m \bmod 2 = 0$ **then**
    $scan\_order \leftarrow 0$ to $N_x - 1$
  else
    $scan\_order \leftarrow N_x - 1$ to 0
  end if
  for n in $scan\_order$ **do**
    $\tilde{f}[m,n] \leftarrow \sum_{k \in \{C,M,Y\}} \tilde{f}_k[m,n]$

$$N_{drop} \leftarrow \begin{cases} 1, & \text{if } \tilde{f}[m,n] < \frac{2}{3} \\ 2, & \text{if } \frac{2}{3} \leq \tilde{f}[m,n] < \frac{4}{3} \\ 3, & \text{if } \frac{4}{3} \leq \tilde{f}[m,n] < 2 \\ 4, & \text{if } 2 \leq \tilde{f}[m,n] < \frac{8}{3} \\ 5, & \text{if } \frac{8}{3} \leq \tilde{f}[m,n] < 3 \\ 6, & \text{if } \tilde{f}[m,n] \geq 3 \end{cases}$$

    $K \leftarrow$ Sorted result of $k \in \{C, M, Y\}$ in in the order of descending absorptance in the current pixel
    $i \leftarrow 0$
    while $N_{drop} > 0$ **do**
      $k \leftarrow K[i]$
      if $\tilde{f}_k[m,n] \geq \frac{2}{3}$ and $N_{drop} \geq 2$ **then**
        $b_k[m,n] = 1$
        $N_{drop} \leftarrow N_{drop} - 2$
      else if $\tilde{f}_k[m,n] \geq \frac{1}{3}$ and $N_{drop} \geq 1$ **then**
        $b_k[m,n] = 0.5$
        $N_{drop} \leftarrow N_{drop} - 1$
      end if
      if $i = 2$ **then**
        break
      end if
      $i \leftarrow i + 1$
    end while
    $e[m,n] = \tilde{f}[m,n] - g[m,n]$
    $\tilde{f}[m+k, n+l] \leftarrow \tilde{f}[m+k, n+l] + e[m,n]h[k,l]$, where $h[k,l]$ is given by Eq. (4)
  end for
end for
return $b_k[m,n]$, $k \in \{C, M, Y\}$

screen blending-in was proposed as a preprocessing step prior to dot-off-dot error diffusion. Blending-in the DBS screened image for dot-off-dot error diffusion results in halftone images without the artifacts associated with error diffusion and smoothness comparable to those generated with simple 2-drop error diffusion or dot-off-dot error diffusion without preprocessing.

References

[1] F. A. Baqai, J.-H. Lee, A. U. Agar, and J. P. Allebach, "Digital color halftoning," *IEEE Signal Proc. Mag.*, vol. 22, no. 1, pp. 87–96, 2005.

[2] T. Frank, A. Jumabayeva, J. P. Allebach, and Y. Yitzhaky, "New design for compact color screen sets for high-end digital color press," *IEEE Trans. Image Process.*, vol. 29, no. 1, pp. 3023–3038, 2020.

[3] R. Ulichney, "The void-and-cluster method for dither array generation," in *Proc. SPIE*, vol. 1913, San Jose, CA, USA, 1993, pp. 332–343.

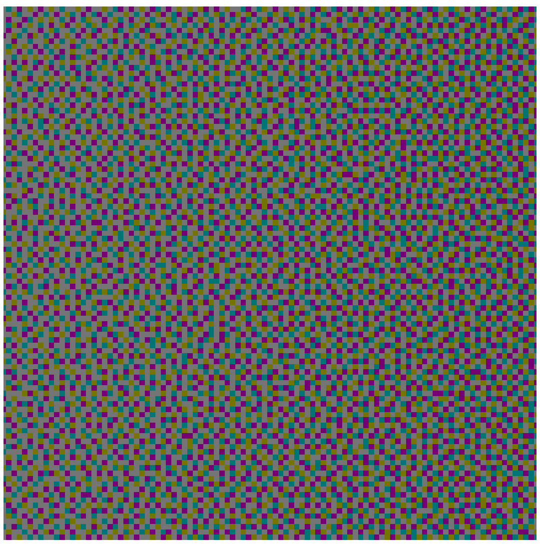

Figure 13. *Halftoned image of Figure 2 using DBS screen blending-in and dot-off-dot 2-drop error diffusion algorithm.*

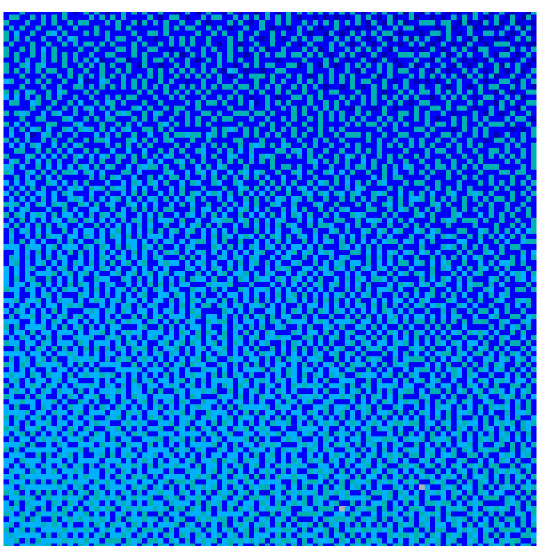

Figure 14. *Halftoned image of Figure 5 using DBS screen blending-in and dot-off-dot 2-drop error diffusion algorithm.*

[4] J. P. Allebach and Q. Lin, "FM screen design using DBS algorithm," in *Proc. IEEE Int. Conf. Image Process.*, Lausanne, Switzerland, 1996, pp. 549–552.

[5] R. W. Floyd and L. Steinberg, "An adaptive algorithm for spatial greyscale," in *Proc. S.I.D.*, vol. 17, no. 2, 1976, pp. 75–77.

[6] D. J. Lieberman and J. P. Allebach, "A dual interpretation for direct binary search and its implications for tone reproduction and texture quality," *IEEE Trans. Image Process.*, vol. 9, no. 11, pp. 1950–1963, 2000.

[7] J.-R. Liao, "Theoretical bounds of direct binary search halftoning," *IEEE Trans. Image Process.*, vol. 24, no. 11, pp. 3478–3487, 2015.

[8] P. Li and J. P. Allebach, "Tone dependent error diffusion," *IEEE Trans. Image Process.*, vol. 13, no. 2, pp. 201–215, 2004.

[9] V. Monga, N. Damera-Venkata, and B. L. Evans, "Design of tone-dependent color-error diffusion halftoning systems," *IEEE Trans. Image Process.*, vol. 16, no. 1, pp. 198–211, 2007.

[10] J.-H. Lee and J. P. Allebach, "Colorant-based direct binary search halftoning," *J. Electron. Imag.*, vol. 11, no. 4, pp. 517–527, 2002.

[11] A. U. Agar and J. P. Allebach, "Model-based color halftoning using direct binary search," *IEEE Trans. Image Process.*, vol. 14, no. 12, pp. 1945–1959, 2005.

[12] Z. He, "Hierarchical colorant-based direct binary search halftoning," *IEEE Trans. Image Process.*, vol. 19, no. 7, pp. 1824–1836, 2010.

[13] M. T. Schramm and J. S. Gondek, "Tone dependent plane dependent error diffusion halftoning," U.S. Patent 6 870 644 B2, Mar. 2005.

[14] W. Jiang, W. Xi, U. Sarkar, R. Ulichney, and J. P. Allebach, "Color halftoning based on Neugebauer Primary Area Coverage," in *Proc. 22nd Color Imag., Displaying, Process., Hardcopy, Appl. IS&T*, Burlingame, CA, USA, 2017, pp. 91–102.

[15] P. Z. Elias, S. Gooran, and D. Nyström, "Multilevel halftoning and color separation for eight-channel printing," *J. Imag. Sci. Technol.*, vol. 60, no. 5, pp. 50 403–1–50 403–9, 2016.

[16] G.-Y. Lin and J. P. Allebach, "Multilevel screen design using direct binary search," *J. Opt. Soc. Am. A (Opt. Image Sci. and Vision)*, vol. 19, no. 10, pp. 1969–1982, 2002.

[17] K. Chandu, M. Stanich, C. W. Wu, and B. Trager, "Direct multi-bit search (DMS) screen algorithm," in *Proc. IEEE Int. Conf. Image Process.*, Orlando, FL, USA, 2012, pp. 817–820.

[18] W. Jiang, A. Veis, R. Ulichney, and J. P. Allebach, "Novel color halftoning algorithm for ink savings," in *Proc. 23rd Color Imag., Displaying, Process., Hardcopy, Appl. IS&T*, Burlingame, CA, USA, 2018, pp. 4291–4297.

[19] R. Ulichney, *Digital Halftoning*. Cambridge, MA, USA: The MIT Press, 1987.

[20] H. R. Kang, *Digital Color Halftoning*. Bellingham, WA, USA: SPIE Press, 1999.

Author Biography

Baekdu Choi received his B.Sc. in electrical and computer engineering from Seoul National University, Seoul, South Korea in 2017 and is currently working on a Ph.D. in electrical and computer engineering at Purdue University, West Lafayette, IN, USA. His research mainly focuses on digital image processing, digital halftoning and color management for inkjet printers.

Daulet Kenzhebalin received his B.S. in computer engineering from Purdue University, West Lafayette, IN, USA in 2015. Currently he is pursuing a Ph.D. in electrical engineering at Purdue University. His primary

area of research has been image processing and machine learning.

Sige Hu received his B.S. in Electrical and Computer Engineering from Pennsylvania State University, State College, PA, USA in 2017 and is currently pursuing Ph.D. in Electrical and Computer Engineering at Purdue University, West Lafayette, IN, USA. His research mainly focuses on image processing.

George T. Chiu is a Professor in the School of Mechanical Engineering with courtesy appointments in the School of Electrical and Computer Engineering and the Department of Psychological Sciences at Purdue University. He also serves as the Assistant Dean for Global Engineering Programs and Partnership for the College of Engineering. Dr. Chiu received the B.S. degree in Mechanical Engineering from the National Taiwan University in 1985 and the M.S. and Ph.D. degrees in Mechanical Engineering from the University of California at Berkeley, in 1990 and 1994, respectively. From September 2011 to June 2014, he served as the Program Director for the Control Systems Program at the National Science Foundation. His current research interests are mechatronics and dynamic systems and control with applications to digital printing and imaging systems, digital fabrications and functional printing, human motor control, motion and vibration perception and control. He received the 2012 NSF Director's Collaboration Award and the 2010 IEEE Transactions on Control System Technology Outstanding Paper Award. He served as the Editor-in-Chief for the IEEE/ASME Transactions on Mechatronics from 2017-19 and as the Editor for the Journal of Imaging Science and Technology from 2012-14. Dr. Chiu served on the Executive Committee of the ASME Dynamic Systems and Control Division (DSCD) from 2007 to 2014 and as the Chair of the Division from 2012-13. He is a Fellow of ASME and a Fellow of the Society for Imaging Science and Technology (IS&T).

Peng (Davi) He is a software manager in Sunvalleytek International Inc, Shenzhen, Guangdong, China. He received his B.S. in Communication Engineering from Hunan University of Arts and Science, Changde, Hunan, China in 2012. His current research interest including artificial intelligence and robot.

Zillion (Zhenqing) Lin is a technical director in Sunvalleytek International Inc, Shenzhen, Guangdong, China. He received his B.S. in Microelectronics Engineering from University of Electronic Science and Technology of China, Chengdu, Sichuan, China in 2008 and M.S. in Biomedical Engineering from Shenzhen University, Shenzhen, Guangdong, China. His current research interest including artificial intelligence and robot.

Jan P. Allebach is Hewlett-Packard Distinguished Professor of Electrical and Computer Engineering at Purdue University. Allebach is a Fellow of the IEEE, the National Academy of Inventors, the Society for Imaging Science and Technology (IS&T), and SPIE. He was named Electronic Imaging Scientist of the Year by IS&T and SPIE, and was named Honorary Member of IS&T, the highest award that IS&T bestows. He has received the IEEE Daniel E. Noble Award and the IS&T/OSA Edwin Land Medal, and is a member of the National Academy of Engineering.